Simulation and Analysis of the Residual Volume of the Drop Impact a Cylinder with a Rhombus Cross Section by Volume of Fluid Method

Javad Alishah[1], Soroush Madah[2*], Javad Alinejad[3], Yaser Rostamian[4]

Abstract– In this article, the impact of a water drop on a horizontal cylinder with a rhombus cross-section is simulated in three dimensions. The innovation of the present work is to investigate the change in the shape of the division and the remaining volume of the collision of a Newtonian droplet with a rhombic cross-section. For the numerical simulation of this phenomenon, the volume of Fluid method based on the dynamic contact angle has been used to track the fluid-solid interface. To validate the results, the impact of a water drop with a diameter of 2 mm at a speed of 1 m/s on a horizontal pipe with a diameter of 3.18 mm and a deviation of 1.55 from the center has been simulated. The simulated images of drop shape change after impact agree well with the experimental results. Then the impact of drops on cylinders with a rhombus section was investigated. The calculation of the remaining and divided volume of the drop shows that the maximum remaining volume of the drop($2.7522 \times 10^{-9} m^3$) is on the cylinder with a diameter of d= 2.4 mm and speed V= 1m/s and the minimum remaining volume of the drop ($0.8391 \times 10^{-9} m^3$) on the cylinder with a diameter of d= 1.6 mm and speed V=2 m/s.

Keywords: Cylinder, rhombic cross-section, residual drop volume, volume of Fluid method

1-Introduction

Deformation and breaking of liquid droplets is observed in a wide range of industrial applications and natural processes. For example, combustion systems of electro spray painting, cosmetic sprays, inkjet printers, turbines and cooling systems are some of the industrial applications. Also, there are many examples in geophysical phenomena from volcanic explosion and rock formation to rain phenomenon. According to the conditions in which the drop is placed. The mechanism of the two-phase system varies from movement in the moving environment to free fall in the stationary environment under the effect of gravity. In 2010, J.Q.feng [1] studied the flows governing a droplet falling at a finite speed using the finite element method. He investigated different values of viscosity and density as well as Reynolds and Weber numbers and calculated the friction coefficient. In 2004, Gottesdiener et al. [2] calculated the stable drop fall speed in different conditions with a similar method, but did not investigate the failure of the drop. J. Han and G.Tryggvasson [3] used the finite difference method to track the unstable movement of drops. studied in different liquids. The results of this research were classified in two density ratios of 1.5 and 10 and different dimensionless numbers. Like most of the numerical research done in this research, only changes in the shape and speed of the drop were discussed and no results were presented for failure. The drop mechanism in the two-phase system is affected by its physical conditions in a static environment under gravity, such as a shock cylinder. Chang et al [4]. experimentally investigated the droplet effect on a cold surface and investigated the energy conversion between the droplet and the environment. Ma and his colleagues [5]. numerically simulated the effect of a three-dimensional drop on supercold and rough surfaces using the Boltzmann lattice method. Kezhao and his colleagues [6] theoretically studied the effect of droplet diffusion on the liquid film, which increased the thickness of the liquid film. Luo and his colleagues [7] numerically investigated the controlled contact time of droplets on solid surfaces. Zhang and his colleagues [8] experimentally investigated the phenomenon of splashing and spreading of droplets on a wettable surface with different diameter and speed of the droplets. Taoli et al. [9] numerically investigated the effect of nanodroplet expansion on surfaces to reduce contact time. Wang et al. [10] used high-speed photography technology Experimentally investigated two drops with low speed on a liquid film. Ma and his colleagues [11] have investigated the impact of three-dimensional simulated metal drops on a dry surface with the hydrodynamics approach of Vsevolodsklabanskyi et al[12]. They theoretically studied the droplet impact in the gas flow by increasing the velocity gradient and its colleagues. YanzhouQin et al[13] numerically investigated the droplet impact in the proton exchange space fuel cell Expansion increases with droplet velocity. Lifan et al [14] numerically simulated the impact of droplets with variable speed on an engross microgroove with variable surface temperature. ZhenyanXia and his colleagues [15] experimentally investigated the effect of water drop on superhydrophobic surface with laser treatment. G. Y. Li and his colleagues [16] numerically investigated the effect of a water drop on a solid surface

1 Department of Mechanical Engineering, Sari Branch, Islamic Azad University, Sari, Iran. Email: Javad.Aalishah@gmail.com

2* Corresponding Author: Department of Mechanical Engineering, Sari Branch, Islamic Azad University, Sari, Iran . Email: S.maddah@iausari.ac.ir

3 Department of Mechanical Engineering, Sari Branch, Islamic Azad University, Sari, Iran. Email: Alinejad_Javad@iausari.ac.ir

4 Department of Mechanical Engineering, Sari Branch, Islamic Azad University, Sari, Iran. Email: yasser.rostamiyan@iausari.ac.ir

Received: 2024.05.29; Accepted: 2024.07.08

with characteristics of heat transfer and smoothed particles. KeisukeUeda and Taylor [17] numerically investigated the impact of nanodroplet with thermodynamic behavior and different diameters in the drug.

2. Governing Equations

The equations governing the multiphase flow are the classic Navier-Stokes equations. The basic rules in fluid mechanics are conservation of mass, momentum and energy. The equilibrium equations of mass and magnitude of motion represent the transition in one phase. In isothermal transfer, heat and energy balance equation is ignored. Because in the current study, the flow is assumed to be calm. There is no need to use turbulent flow models.

$$\nabla.U = 0 \quad (1)$$

$$\frac{\partial(\rho U)}{\partial t} + \nabla.(\rho UU) = -\nabla p + \nabla.T + \rho f_b \quad (2)$$

where the velocity vector and $T = 2\mu S - 2\mu(\nabla.U)\delta_{i,j}/3$ are the viscous stress tensor. Also $S = 0/5\left[\nabla U + (\nabla U)^T\right]$ in the stress tensor represents the tensor of the average rate of gravity, $\delta_{i,j}$ the symbol of Kroner's delta, which is equal to one for thermal stress components (i=j) and zero in cases (i≠j). P The pressure, ρ density and f_b It represents the volumetric forces in the unit of mass, which includes the forces of gravity and surface tension in the interface. In the fluid volume method, the variable γ is used to describe the volume fraction of each phase in a cell as a function of space Time is defined. In this method, the volume fraction transfer equation is solved simultaneously with the continuity and motion equations (18).

$$\frac{\partial\gamma}{\partial t} + \nabla.(U\gamma) = 0 \quad (3)$$

The volume fraction γ is in the range of $0 \le \gamma \le 1$ and the values of 0 and 1 correspond to the areas occupied by only one phase.

$$\frac{\partial\gamma}{\partial t} + \nabla.(U_l\gamma) = 0 \quad (4)$$

$$\frac{\partial(1-\gamma)}{\partial t} + \nabla.\left[U_g(1-\gamma)\right] = 0 \quad (5)$$

where his subscripts L and g represent the liquid and gas phases respectively. Assuming that the contribution of liquid and gas velocities in the assessment of the free surface is proportional to the corresponding volume fraction and also the effective fluid velocity in the fluid volume method as an average Weight is defined as follows

$$U = \gamma U_l + (1-\gamma)U_g \quad (6)$$

And by inserting the above equation in the volume fraction equation (3) we will have.

$$\frac{\partial\gamma}{\partial t} + \nabla.\left\{\left[\gamma U_l + (1-\gamma)U_g\right]\gamma\right\} = 0 \quad (7)$$

By defining the relative speed as compression speed as follows:

$$U_r = U_l - U_g \quad (8)$$

And by substituting the above equation in equation (7), we will have:

$$\frac{\partial\gamma}{\partial t} + \nabla.\left\{\left[U_l - (1-\gamma)U_r\right]\gamma\right\} = 0 \quad (9)$$

By rearranging the above equation, we will have:

$$\underbrace{\frac{\partial\gamma}{\partial t} + \nabla.(U_t\gamma)}_{=0} - \nabla.\left\{\left[(1-\gamma)\gamma U_r\right]\right\} = 0 \quad (10)$$

According to the definition of the transfer equation in the liquid phase, the two terms on the left side of the above equation are equal to zero. So we will have:

$$\nabla.\left[(1-\gamma)\gamma U_r\right] = 0 \quad (11)$$

Now, by adding this expression in the transfer equation, we will have a volume fraction:

$$\frac{\partial\gamma}{\partial t} + \nabla.(U\gamma) + \nabla.\left[U_r\gamma(1-\gamma)\right] = 0 \quad (12)$$

In short, the present mathematical model is defined by the continuity equations of motion size and fuzzy fraction.

3. Dynamic contact angle

The contact angle between the droplet phase and the solid cylinder is simulated and calculated in Figure 1. The vector perpendicular to the surface curvature for the fluid phase (droplet) $\hat{n}_d$ and the solid phase of solid cylinders) $\hat{n}_t$ is shown as follows:

$$\hat{n}_d = \frac{\nabla\alpha}{|\nabla\alpha|} \quad (13)$$

$$\hat{n}_t = \frac{\nabla(1-\Phi)}{|\nabla(1-\Phi)|} \quad (14)$$

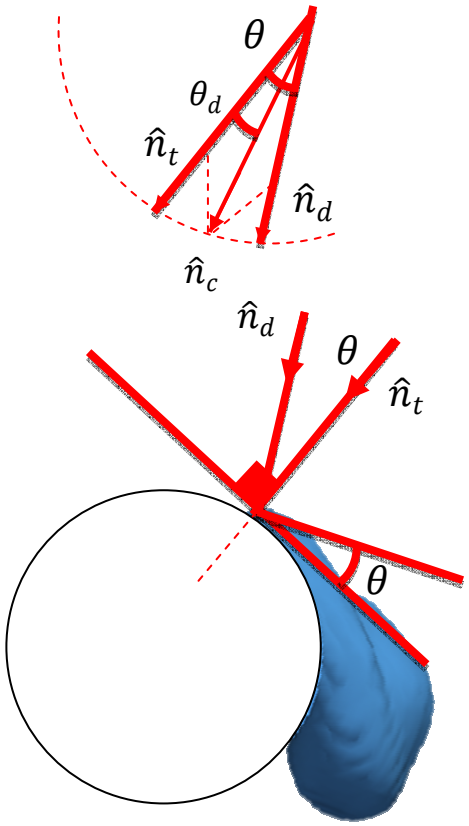

Fig. 1 Schematic view of the contact angle between the drop and the cylinder

The spatial angle (θ) between two vectors perpendicular to the curvature of the interface between solid and fluid is as follows:

$$\boldsymbol{\cos(\theta) = \hat{n}_d . \hat{n}_t} \quad (15)$$

The three-dimensional interface between the fluid phase (droplet) and solid phase (of solid cylinders) with vectors perpendicular to each of the phases and n_c

$$\boldsymbol{\hat{n}_c = \frac{\sin(\theta_d)}{\sin(\theta)} \hat{n}_d . \frac{\sin(\theta - \theta_d)}{\sin(\theta)} \hat{n}_t} \quad (16)$$

It is given that they are shown using the contact line n_c and are expressed as follows:

where is the dynamic contact angle of the drop on solid cylinders as shown in Figure 1. For water droplets on a stainless steel surface, the advance and equilibrium contact angles are calculated as 40, 110 and 75, respectively.

4. Independence from the network

The quality of the mesh size has been evaluated by changing the ratio of the number of cells to the droplet radius (cpr). The pressure jump of P level at the interface of two fluids is calculated for comparison. Therefore, the compressive stress equation is shown as follows:

$$p_s^c = \frac{\sum_{i.j.k} f_{i.j.k} p_{i.j.k}}{\sum_{i.j.k} f_{i.j.k}} \quad (17)$$

where $f_{i,j,k}$ and $p_{i,j,k}$ are the volume fraction and pressure of a cell in the two-fluid domain, respectively. Therefore, the tensile stress error toThe following is shown:

$$E = \frac{p_s^c}{4\sigma/D} - 1 \quad (18)$$

That σ and D show the surface tension of the fluid (air-liquid) and the droplet diameter, respectively. According to Figure (2), the errors relative to the number of cells for cpr=15are less than %5 and close to Cpr = 18 and the current simulation is based on cpr= 15.

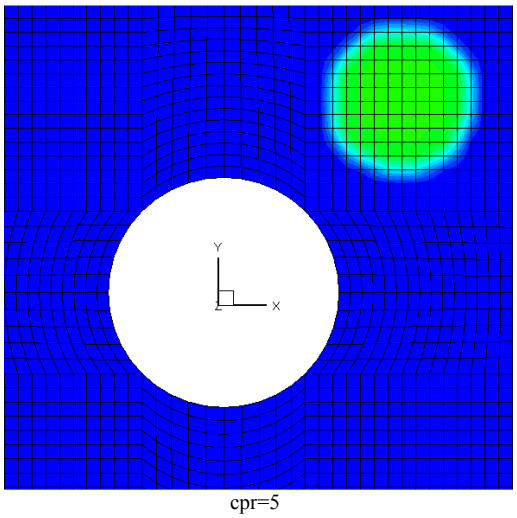

cpr=5

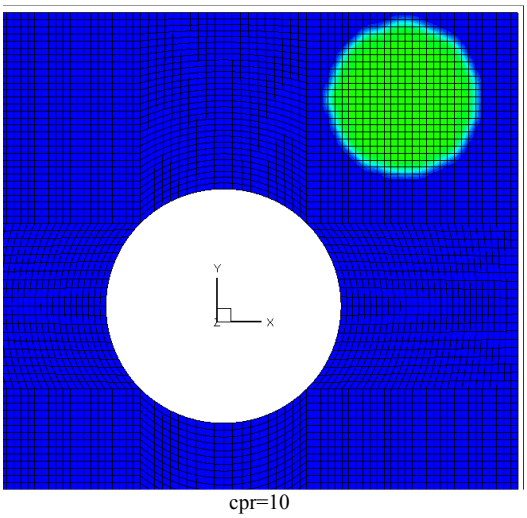

cpr=10

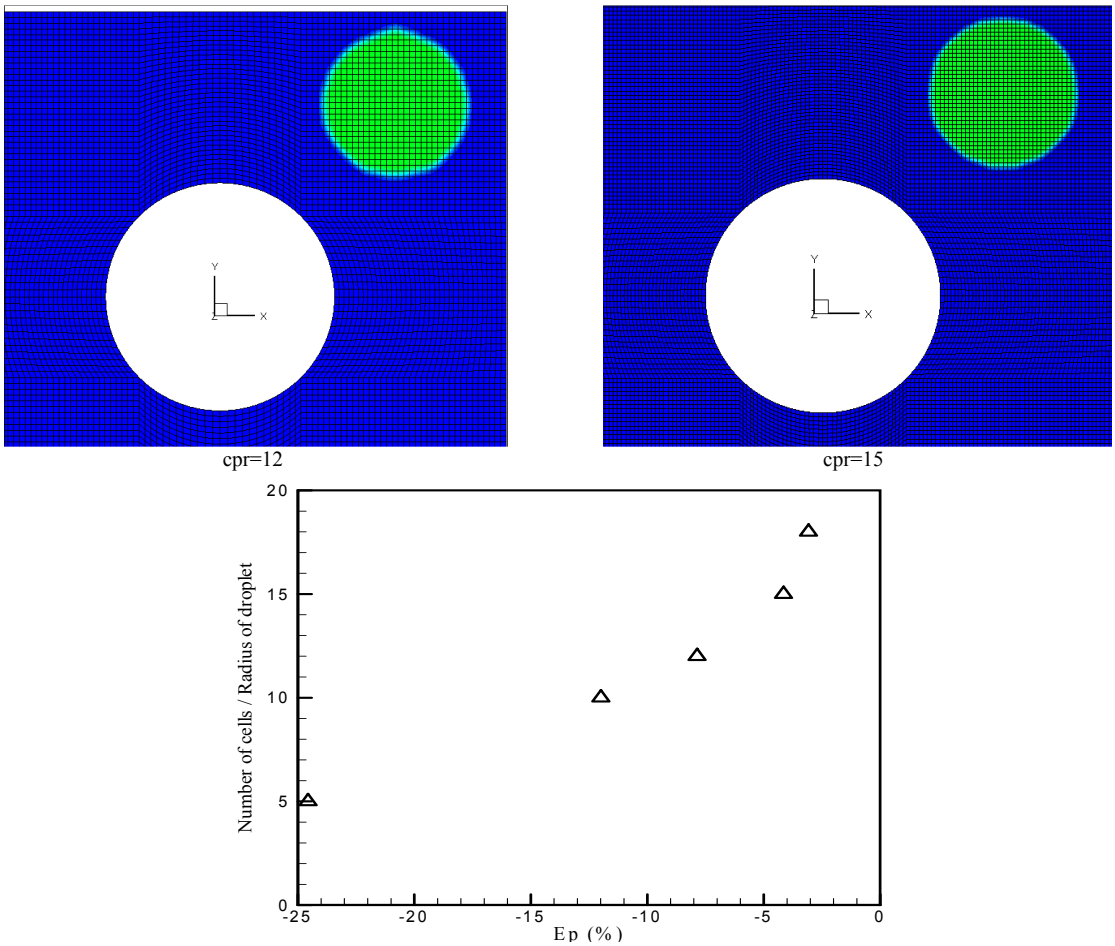

Fig.2. Error percentage in relation to the number of cells to droplet radius (cpr)

5. Validation

Figure 3 shows the impact of a water droplet with a speed of 1 m/s and a diameter of 2 mm on a steel pipe with a diameter of 3.18 mm (0.125 inch). The center of the drop deviates 1.55 mm from the center line of the tube. Figure 3 shows the successive stages of the change of the shape of the droplet along the axis of the tube. The time of each frame is measured from the moment when the droplet touches the tube for the first time. Experimental photos [19] have a very good match with the images produced by the computer model.

Exprimental result [19]

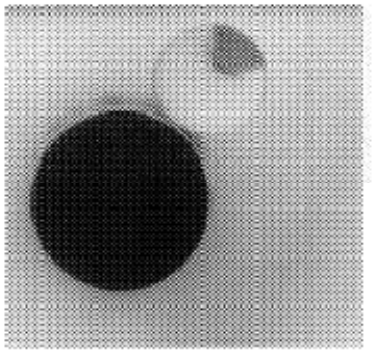

Present study

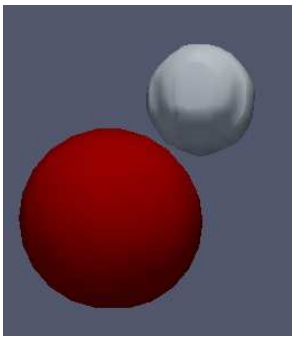

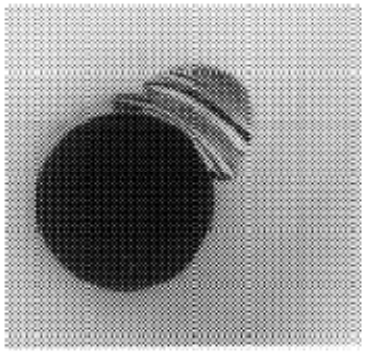

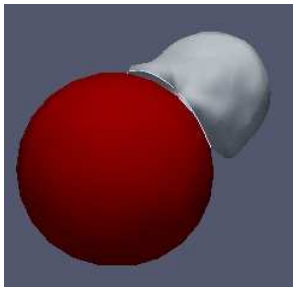

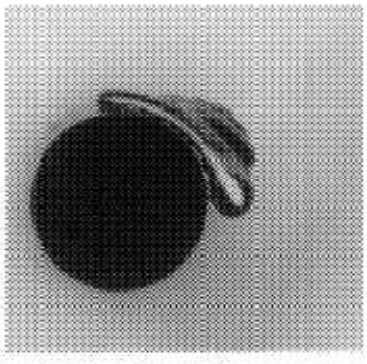

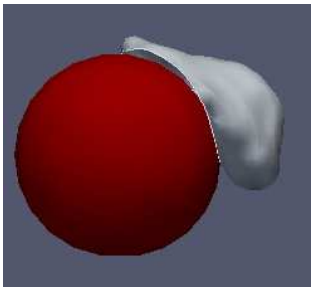

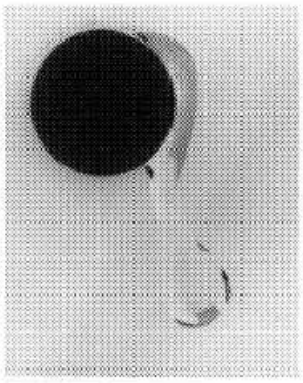

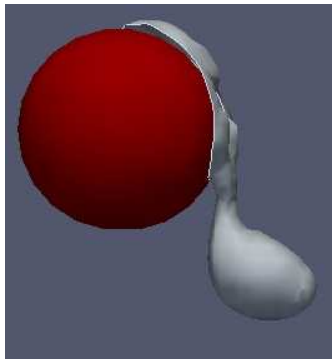

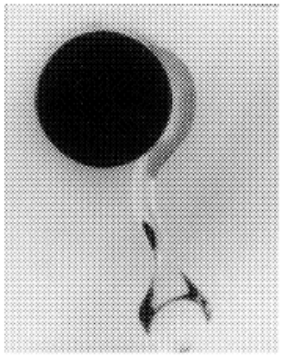

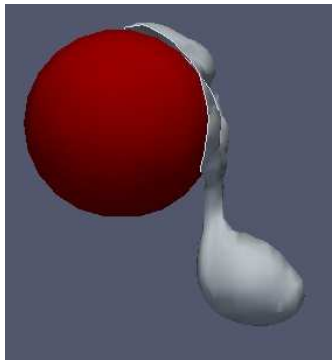

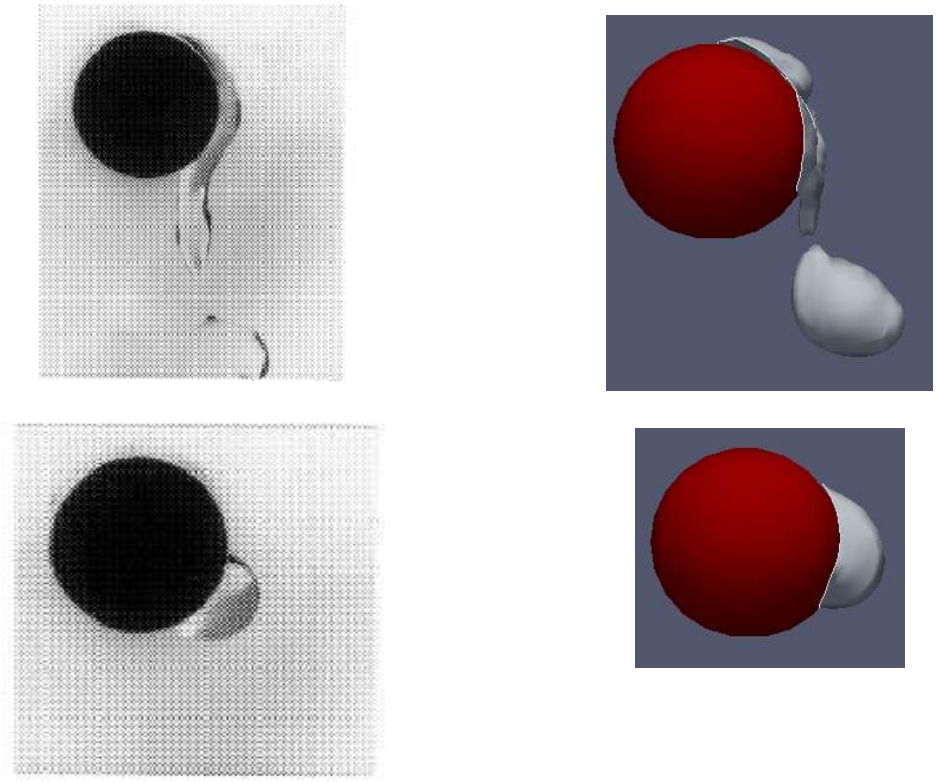

Fig. 3 . Comparison of simulation results from the side view of a drop of water hitting a steel pipe

6. Results

The present study numerically investigates the impact of a three-dimensional Newtonian drop on a pipe with a rhombic section. These results examine the changes of drop diameter in d= 2.4, 2 and 1.6 mm and drop speed of 1 and 2 m/s. Figure 4 shows the impact of drops with a diameter of 2 and 2.4 mm and a speed of 1 m/s on a pipe with a rhombus section at different times. The physical factors effects and the behavior analysis of the droplet impact on rhombus cylinder were investigated. Break droplets deformation are simulated using the volume of fluid (VOF) method with open-source software based on the droplet's dynamic contact angle at the spatial interface between two solid-fluid phases. Finally, some of the main points summarized:

- The reduction of time costs in simulating this phenomenon, which is much less CPU time consuming than previous researches.
- Analysis of break of droplet on cylinders with different physical conditions using changing in remaining volume of droplet.
- Survey of effect of droplet diameter into cylinder dimension on the number of broken droplets.
- In case that droplet diameter is big and the velocity is small, the Volume percentage of passing droplet is maximum.

Table 1. Comparison between the relaxation time of the droplet on the cylinder and the remaining volume of the droplet on the cylinder for impactIt shows the drop with different speeds on the cylinder with a rhombus section.

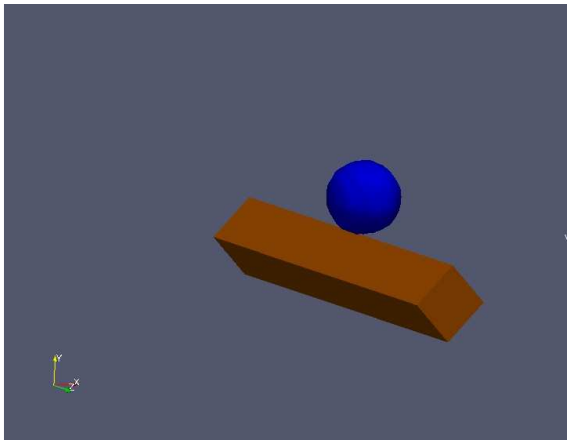

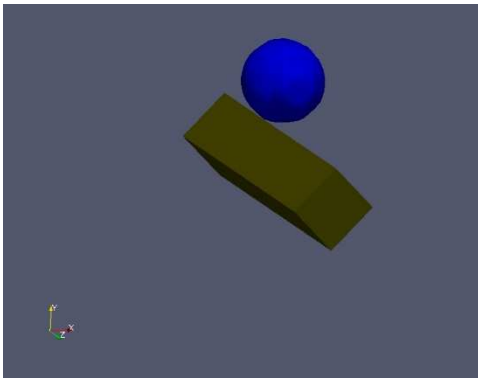

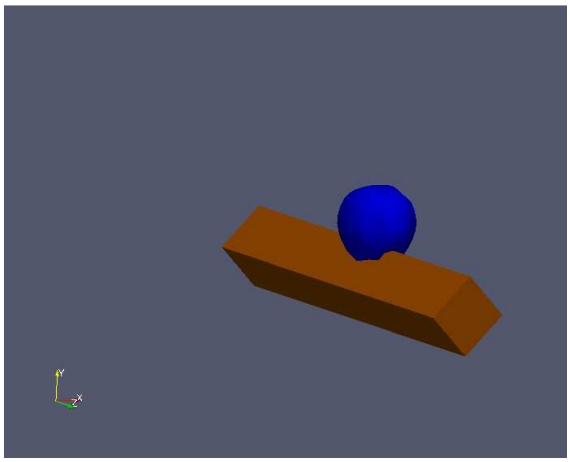

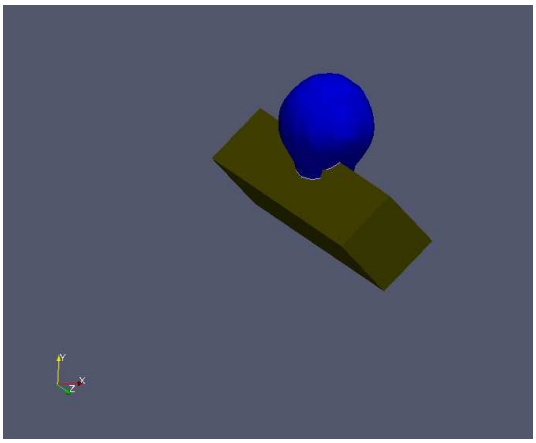

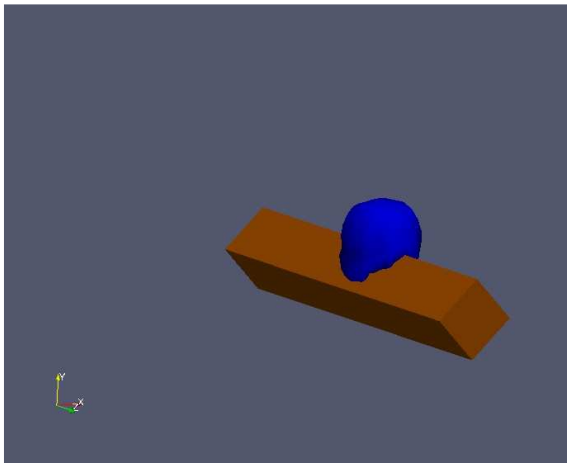

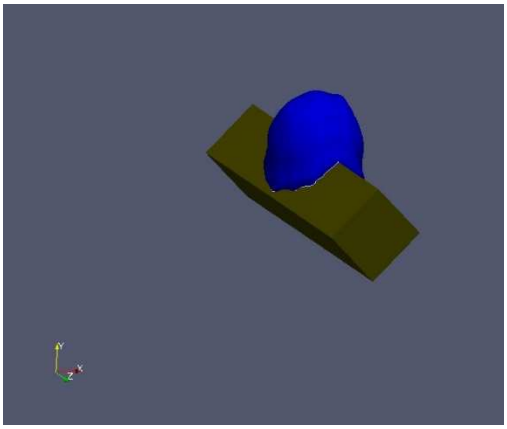

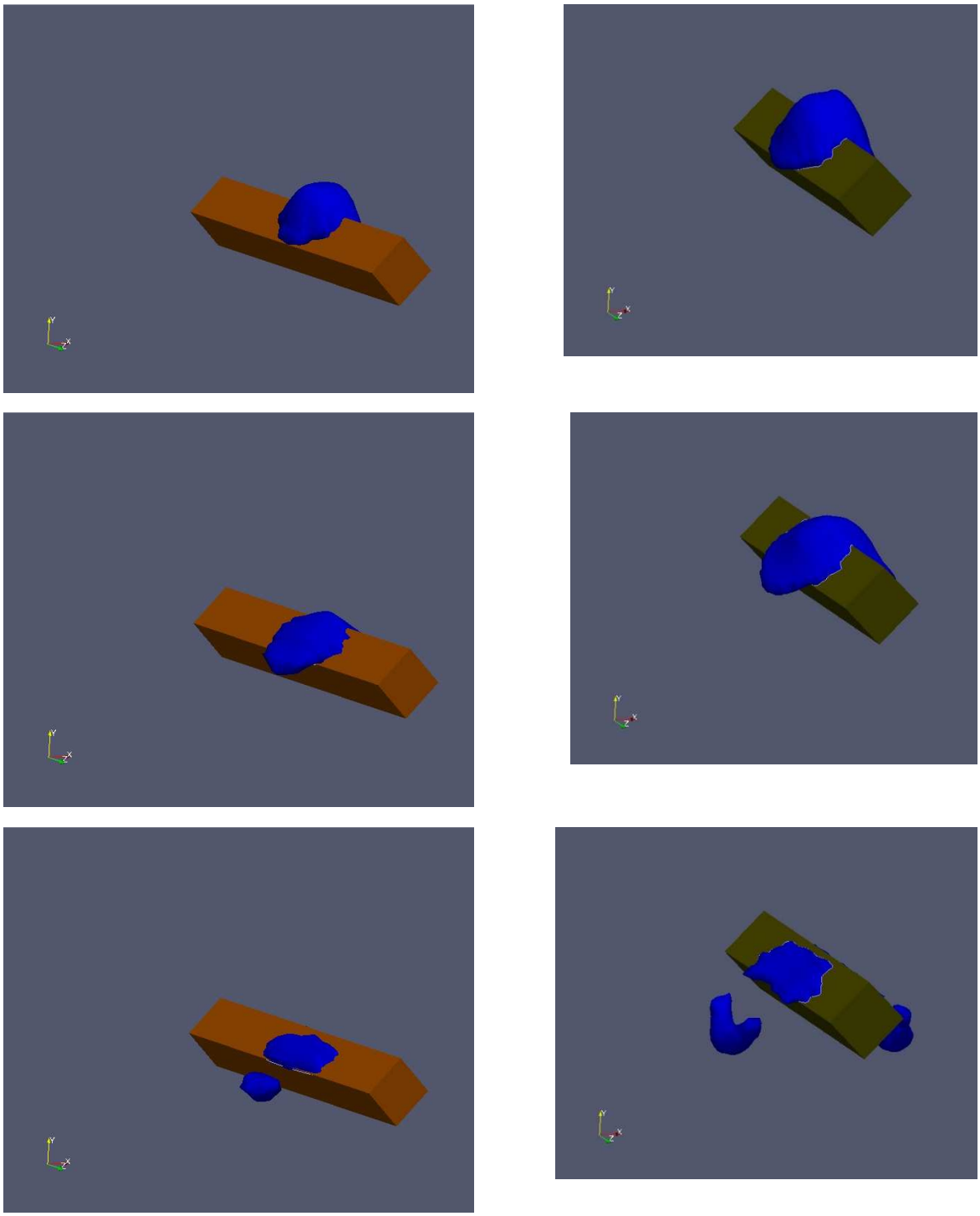

Fig. 4. Simulation results of a drop of water hitting a steel pipe with a rhombus section

Table 1. Comparison between droplet behaviors in all modes

Volume percentage of passing drop	remaining volume Drop on the tube ($\times 10^{-9}m^3$)	falling speed (m/s)	Drop specifications
62 %	2.7522	1	d = 2.4 mm
78 %	1.5546	2	d = 2.4 mm
59 %	1.7173	1	d = 2 mm
71 %	1.2146	2	d = 2 mm
54 %	0.9819	1	d = 1.6 mm
60 %	0.8391	2	d = 1.6 mm

7. Conclusion

In this article, the impact of a drop on a solid tube with a rhombus cross-section is simulated using the volume of fluid method based on the dynamic contact angle of the drop, so the impact and change of shape of a drop with diameters of d= 1.6,2.2and 2.4 and drop velocities at V=1m/s and 2 m/s around the cylinder were calculated and the remaining volume of the drop and the volume passed through the tube were investigated.

Is. Finally, some important points are summarized as follows:

- The comparison of the broken volume of the drop shows that the lowest percentage of the passing volume of the drop is %54 The drop was d= 1.6 mm and the speed was 1 m/s.
- The maximum remaining volume of the drop is 2.7522 x 10^{-9}m^3, corresponding to the drop with a diameter of d = 2.4 mm and V =1 m/s.
- The highest percentage of passing volume of the drop, %78, corresponds to the drop with a diameter of d= 2.4 mm and d=2 m/s.
- The minimum remaining volume of the drop is 0.8391×10^{-9}m^3 corresponding to the drop with a diameter of d = 1.6 mm and a speed of V=2 m/s.

English signs	
t	time (s)
Δt	time step
T	Viscous stress tensor
f_b	Body force per unit mass
P	Pressure
S	Average strain rate tensor
Ur	Compression speed
$\hat{n}_d$	The vector perpendicular to the surface curvature for the fluid phase
$\hat{n}_t$	The vector perpendicular to the surface curvature for the solid phase
P_S^C	Compressive stress
E	Tensile stress error
D	Droplet diameter (m)
cpr	The number of cells per droplet radius
f	Fluid fraction volume
I,j,k	Coordinates
List of Greek symbols	
ρ	Density (kg/ m^3)
μ	Viscosity
γ	Phase volume fraction
Φ	Fluid phase volume fraction
θ	The spatial angle between $\hat{n}_t$ and $\hat{n}_d$
σ	Surface tension
δ_{ij}	Kronecker Delta
θ_d	Drop dynamic contact angle

References

[1] J. Q. Feng, "A deformable liquid drop falling through a quiescent gas at terminal velocity", J. Fluid Mech, 2010, 658, 438-462.

[2] L. Gottesdiener, D. Gueyffier, M. Abdelouahab, R.Gatignol, and S. Zaleski, "Numerical simulations of large falling drops", Int. J . Mum. Methods Fluids, 2004, 45(1), 109-123.

[3] J. Han and G. Tryggvasson, "Secondary breskup of axisymmetric liquid drops. I. Acceleration by a constant body force" , Phys. Fluids, 1999, 11(12), 36-50.

[4] ShinanChang, HeSong, KeWu, "Experimental investigation on impact dynamics and freezing performance of water droplet on horizontal cold surface," Sustainable Energy Technologies and Assessments, Vol. 45, 101128, 2021.

[5] Zhiyuan Ma, W.Xiong, P.Cheng, "3D Lattice Boltzmann simulations for water droplet's impact and transition from central-pointy icing pattern to central-concave icing pattern on super cooled surfaces. Part II: Rough surfaces," International Journal of Heat and Mass Transfer, Vol. 172, 121153, 2021.

[6] KeZhao, YuWang, YangDing, YanlongJiang, "Numerical and theoretical study on the spreading characteristics of droplet impact on a horizontal flowing liquid film," Colloids and Surfaces A: Physicochemical and Engineering Aspects, Vol. 616, 126338, 2021.

[7] JiaLuo, Shuang-YingWu, LanXiao, Zhi-LiChen, "Parametric influencing mechanism and control of contact time for droplets impacting on the solid surfaces," International Journal of Mechanical Sciences, Vol. 197, 106333, 2021.

[8] HaixiangZhang, XiwenZhang, XianYi, FengHe, Fenglei Niu, PengfeiHao, "Effect of wettability on droplet impact: Spreading and splashing," Experimental Thermal and Fluid Science, Vol. 124, 110369, 2021.

[9] TaoLi, LishuZhang, MingyuLid, MengYan, ErliNi, YingRuan, HuiLi, "Non-retraction rebound of the impacting nano-droplets," Journal of Molecular Liquids, Vol. 329, 115521, 2021.

[10] JiajunWang, GangtaoLiang, TianjiaoWang, YiZheng, HaibingYu, ShengqiangShen, "Interfacial phenomena in impact of droplet array on liquid film," Colloids and Surfaces A: Physicochemical and Engineering Aspects, Vol. 615, 126292, 2021.

[11] TianyuMa, DaweiChen, HaiquanSun, DongjunMa, AiguoXu, PeiWang, "Dynamic behavior of metal droplet impact on dry smooth wall: SPH simulation and splash criteria," European Journal of Mechanics - B/Fluids, in press, 2021.

[12] VsevolodSklabinskyi, IvanPavlenko, "Intensification of mass transfer processes through the impact of the velocity gradient on hydrodynamics and stability of liquid droplets in a gas flow," Chemical Engineering Science, 235, 116470, 2021.

[13] YanzhouQin, QiaoyuGuo, RouxianChen, YuanZhuang, YulinWang, "Numerical investigation of water droplet impact on PEM fuel cell flow channel surface," Renewable Energy, Vol. 168, pp. 750-763, 2021.

[14] Yee LiFan, ZhibingZhan, ChunleiGuo, Jeong-HyunKim, JinkeeLee, "Retraction dynamics of a water droplet impacting onto a micro grooved hydrophobic surface at different velocities and surface temperatures," International Journal of Heat and Mass Transfer, Vol. 168, 120851, 2021.

[15] ZhenyanXia, YangZhao, ZhenYang, ChengjuanYang, LinanLi, ShibinWang, MengWang, "The simulation of droplet impact on the super-hydrophobic surface with micro-pillar arrays fabricated by laser irradiation and salinization processes," Colloids and Surfaces A: Physicochemical and Engineering Aspects, Vol. 612, 125966, 2021.

[16] G.Y.Li, X.J.Ma, B.W.Zhang, H.W.Xu, "An integrated smoothed particle hydrodynamics method for numerical simulation of the droplet impacting with heat transfer," Engineering Analysis with Boundary Elements, Vol. 124, p.p. 1-13, 2021.

[17] KeisukeUeda, Lynne S.Taylor, “Partitioning of surfactant into drug-rich nanodroplets and its impact on drug thermodynamic activity and droplet size,” Journal of Controlled Release, Vol. 330, p.p. 229-243, 2021.

[18] C. W. Hirt and B. D. Nichols, Volume of fluid (VOF) method for the dynamics of free boundaries", J. Comput. Phys., 1981039, 201.

[19] Pasandideh-Fard M, Bussmann M, Chandra S, Mostaghimi, J (2001) Simulating Droplet Impact On a Substrate of Arbitrary Shape. Atomization Sprays 11(4):397–414.